ELSEVIER

Chemical Engineering Journal 88 (2002) 53–58

Chemical Engineering Journal

www.elsevier.com/locate/cej

Dissolution kinetics of crystals in suspension and its application to L-aspartic acid crystals

Gu Shan, Koichi Igarashi, Hiroshi Ooshima*

Department of Bioapplied Chemistry, Graduate School of Engineering, Osaka City University, 3-3-138 Sugimoto, Sumiyoshi-ku, Osaka 558-8585, Japan

Received 17 April 2001; received in revised form 20 September 2001; accepted 10 October 2001

Abstract

The kinetics of the dissolution of L-aspartic acid crystals under the gentle and vigorous agitation was investigated. A dissolution rate equation was derived by assuming two steps: the disintegration of molecules from the surface of crystals and the mass transfer of disintegrated molecules into the bulk solution. An intrinsic expression of the relationship between the solute concentration of the bulk solution and the dissolution time was also derived. The dissolution process of monodisperse and polydisperse crystals of L-aspartic acid was well estimated, and the change of crystal size distribution of polydisperse crystals during dissolution was simulated with good accuracy.

Keywords: Dissolution kinetics; Agitation; Change in crystal size distribution; Dissolution of L-aspartic acid crystals

1. Introduction

Mechanisms of dissolution kinetics of crystals have been intensively studied in the pharmaceutical domain, because the rate of dissolution affects the bioavailability of drug crystals. The importance of dissolution kinetics is not, however, confined to the pharmaceutical industry but the dissolution kinetics also has important implications in industrial crystallization processes. For example, the dissolution of fine crystals is effective for the production of large crystals with narrow size distribution [1,2]. Moreover, the solvent-mediated transformation of crystal polymorphs involves the process of dissolution of metastable crystals [3].

Many efforts have been made to describe the crystal dissolution behavior. Noyes and Whitney [4] expressed the dissolution rate by assuming that the process is diffusion controlled and involves no chemical reaction. Their equation simply expresses that the dissolution rate is directly proportional to the difference between the solubility and the solution concentration. Dressman and Fleisher [5] developed an expression based on the Noyes–Whitney equation, where the dissolution rate was expressed as a function of the remaining surface area of the crystal and the concentration gradient across the boundary layer. Hintz and Johnson [6] and Lu et al. [7] used the same dissolution rate expression, assuming a mass transfer controlled process, to simulate the dissolution of drugs in polydisperse powder form. These latter studies were made to deal with the oral absorption of drugs.

In industrial crystallization, not only mass transfer but also surface reaction (disintegration of crystals) must be taken into account in order to understand the dissolution process because industrial crystallization is not always carried out under gentle agitation. However, there are only few reports dealing with the effect of the surface reaction rate on the dissolution rate (see e.g. [8]).

In this paper, we examine the dissolution kinetics of crystals in suspension by taking into account the effects of the surface reaction and mass transfer. An analytical equation describing the relationship between the solute concentration and the dissolution time was obtained. Based on our analytical equation, the dissolution rate constant of L-aspartic acid crystals was determined. Furthermore, the change of CSD of polydisperse L-aspartic crystals during dissolution process was simulated in success.

2. Kinetics of crystal dissolution

We assume a consecutive process for crystal dissolution as presented in Fig. 1. First, crystals are disintegrated at the crystal surface, and then the solute diffuses from the surface to the bulk solution. This is the reverse process of crystal growth. Assuming that the disintegration rate r_d and the diffusion rate r_{dif} are proportional to a, being the surface

* Corresponding author. Tel.: +81-6-6605-2700; fax: +81-6-6605-2701.
E-mail address: ooshima@bioa.eng.osaka-cu.ac.jp (H. Ooshima).

1385-8947/02/$ – see front matter
PII: S1385-8947(01)00259-5

Nomenclature

a	surface area of crystals per unit volume of solution ($cm^2\ cm^{-3}$)
C_b	concentration at the bulk solution ($mg\ cm^{-3}$)
C_s	concentration at the surface of crystals ($mg\ cm^{-3}$)
C_{sol}	solubility of solution ($mg\ cm^{-3}$)
E_a	activation energy ($kJ\ mol^{-1}$)
F_i	weight fraction of crystals classified in ith fraction (–)
k	dissolution rate constant ($cm\ min^{-1}$)
k_d	disintegration rate constant ($cm\ min^{-1}$)
k_{dif}	diffusion rate constant ($cm\ min^{-1}$)
k_{obs}	appearance dissolution rate constant ($cm^2\ min^{-1}\ mg^{-2/3}$)
L	size of crystal at any time (cm)
L_0	initial size of crystal (cm)
N_i	number of crystal in the ith fraction (–)
N_0	initial number of crystal (–)
r	diffusion rate ($mg\ cm^{-3}\ min^{-1}$)
r_d	disintegration rate ($mg\ cm^{-3}\ min^{-1}$)
r_{dif}	diffusion rate ($mg\ cm^{-3}\ min^{-1}$)
t	dissolution time (min)
T	absolute temperature (K)
V	volume of dissolution medium (cm^3)
V_P	volume of a particle (cm^3)
w	mass of crystal at any time (mg)
w_0	initial mass of crystal (mg)

Greek letter

ρ	density of the crystal ($mg\ cm^{-3}$)

area of the remaining crystals per unit volume of solution, and the difference of concentration as a driving force, we obtain two equations as follows:

$$r_d = k_d a(C_{sol} - C_s) \tag{1}$$

$$r_{dif} = k_{dif} a(C_s - C_b) \tag{2}$$

where C_s is the concentration of solute at the surface of crystals which is less than the solubility C_{sol}, C_b the concentration of solute in the bulk solution. We also assume that under quasi-steady state condition, the dissolution rate r is equal to the disintegration rate and the diffusion rate, namely,

$$r = -\frac{dw}{V\,dt} = r_d = r_{dif} \tag{3}$$

where w is the mass of the remaining crystals, and V and t are the volume of solution and the dissolution time, respectively. A combination of Eqs. (1)–(3) gives

$$r = -\frac{dw}{V\,dt} = ka(C_{sol} - C_b) \tag{4}$$

$$k = \frac{1}{1/k_d + 1/k_{dif}} \tag{5}$$

where k is the dissolution rate constant. The mass of remaining crystals can be written from mass balance as follows, if $C_b = 0$ at $t = 0$:

$$w = w_0 - C_b V \tag{6}$$

where w_0 is the initial mass of crystals. Combining Eqs. (4) and (6),

$$r = \frac{dC_b}{dt} = ka(C_{sol} - C_b) \tag{7}$$

If the shape of crystals can be characterized using volume shape factor α and surface shape factor β, then

$$a = \frac{\beta L^2 N_0}{V} \tag{8}$$

$$N_0 = \frac{w_0}{\rho V_p} = \frac{w_0}{\alpha\rho L_0^3} \tag{9}$$

where L is the size of crystals at any time and L_0 their initial size, and N_0 the initial number of crystals, which is assumed not to change over the time course of dissolution. V_p is the volume of a particle and ρ the density of the crystal. L can therefore be expressed as follows:

$$L = \left(\frac{w}{\alpha\rho N_0}\right)^{1/3} \tag{10}$$

Substituting Eqs. (9) and (10) into Eq. (8), we obtain

$$a = \frac{\beta C_{all}^{1/3}}{\alpha\rho L_0}(C_{all} - C_b)^{2/3} \tag{11}$$

$$C_{all} = \frac{w_0}{V} \tag{12}$$

C_{all} is the concentration when the initial crystals are completely dissolved. Substituting Eq. (11) into Eq. (7), we obtain

$$\frac{dC_b}{dt} = k_{obs}(C_{all} - C_b)^{2/3}(C_{sol} - C_b) \tag{13}$$

$$k_{obs} = \frac{\beta k}{\alpha\rho L_0} C_{all}^{1/3} \tag{14}$$

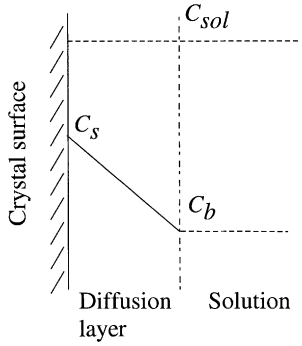

Fig. 1. Dissolution model.

If the crystals are considered to be spherical, $\beta/\alpha = 6$,

$$k_{obs} = \frac{6k}{\rho L_0} C_{all}^{1/3} \tag{15}$$

where L_0 corresponds to the diameter of the crystals.

When $k_d \gg k_{dif}$, Eq. (13) becomes the same as the Noyes–Whitney-type equation [5,6]. The previous authors [5,6] solved Eq. (13) numerically to calculate the dissolution amount as a function of time. We obtained an analytical equation to express the relationship, such that integration of Eq. (13) gives

$$t = \frac{1}{k_{obs} x^2}\left[\ln\left(\frac{x-y}{x-z}\right)\left(\frac{x^2+xy+y^2}{x^2+xz+z^2}\right)^{1/2} + \sqrt{3}\left\{\tan^{-1}\left(\frac{x+2y}{-\sqrt{3}x}\right) - \tan^{-1}\left(\frac{x+2z}{-\sqrt{3}x}\right)\right\}\right],$$
$$x = (C_{all} - C_{sol})^{1/3}, \quad y = (C_{all} - C_b)^{1/3}, \quad z = C_{all}^{1/3} \tag{16}$$

Eq. (16) expresses the change of solute concentration during dissolution.

3. Experiments

3.1. Solubility of L-aspartic acid

L-Aspartic acid used was of reagent grade and purchased from Wako Pure Chemical Industries, Japan. The concentration of L-aspartic acid was determined from UV absorption at 210 nm. The solubility of L-aspartic acid in water was determined by dissolving crystals in water over the temperature range from 5 to 60 °C.

3.2. Dissolution of monodisperse crystals of L-aspartic acid

L-Aspartic acid crystals were precipitated from an aqueous supersaturated solution using a jacketed glass batch crystallizer with a working volume of 200 ml at 20 °C. The crystals were dried on air and sieved into six fractions with sizes of 37–53, 53–74, 74–105, 105–297, 297–420 and 420–500 μm. The classified crystals were regarded as a monodisperse powder with an average size L between the upper and lower sieves.

The dissolution of crystals was carried out in the same vessel described above as a crystallizer. L-Aspartic acid crystals (2.5 g) from one of the classified groups described above was quickly added to 200 ml of water adjusted at a given temperature between 15 and 45 °C and agitated at a given speed between 200 and 1200 rpm. At regular intervals, the slurry was withdrawn and immediately filtered through a membrane filter (pore size 0.1 μm), and then the concentration of the filtrate was determined.

3.3. Determination of dissolution rate constant k

First, the apparent dissolution rate constant k_{obs} was determined by curve fitting using Eq. (16) for the time course of dissolution of monodisperse crystals. The dissolution rate constant k was then determined according to Eq. (15).

3.4. Dissolution of polydisperse crystals of L-aspartic acid

A polydisperse powder with a broad size distribution was prepared by mixing classified crystals of different size L. Dissolution of 2.5 g of the crystals at 25 °C and 500 rpm was initiated in the same way as in the dissolution of monodisperse crystals. The sample crystals were withdrawn at dissolution time of 0.5, 1.0, 1.5, and 3.0 min and immediately filtered through a 0.1 μm pore membrane filter. The filtrate was used to determine the concentration of L-aspartic acid. Crystals on the filter were washed several times with a small amount of methanol. This prevented agglomeration of crystals. The washed crystals were then carefully transferred onto a watch glass and dried at room temperature for 12 h.

3.5. Determination of crystal size distribution (CSD)

The size distribution of polydisperse crystals was determined during the dissolution by image analyzing technique, because the amount of crystals withdrawn from the dissolver was small and the image analysis provides a high-resolution of CSD. In the image analysis, the area of the plane of each crystal A_c was measured and the square root of A_c was regarded as the crystal size L_{image}, i.e. $L_{image} = A_c^{0.5}$. In order to calibrate the relationship between L_{image} determined by the image analysis and L determined from sieving, the sieved crystals were assayed by the image analysis.

The ith fraction of the weight basis CSD, F_i, was calculated as follows:

$$F_i = \frac{L_i^3 N_i}{\sum_{i=1} L_i^3 N_i} \tag{17}$$

where N_i is the number of crystals belonging to the ith fraction.

3.6. Simulation of the change in CSD of polydisperse crystals during dissolution

Polydisperse crystals of L-aspartic acid were classified into 50 size fractions between 100 and 500 μm, i.e. i = 1–50. Changes in the CSD and bulk concentration C_b were simultaneously estimated by a computer calculation as follows.

1. Substituting the experimentally determined k value into Eq. (13), an increment of the bulk concentration $\Delta C_{b,i}$ through the dissolution of ith fraction during the time

increment Δt (=0.01 s) at a dissolution time t was calculated according to the following equation:

$$\Delta C_{b,i} = \Delta C_{b,i,t+\Delta t} - \Delta C_{b,i,t} = k_{obs}(C_{all,i} - C_{b,i,t})^{2/3}(C_{sol} - C_{b,t})\Delta t \quad (18)$$

where $C_{b,t} = \sum_{i=1}^{50} C_{b,i,t}$.

2. Increment $\Delta C_{b,i}$ from each fraction was summed to obtain the bulk concentration, i.e. $C_{b,t+\Delta t}$, as follows:

$$C_{b,t+\Delta t} = C_{b,t} + \sum_{i=1}^{50} \Delta C_{b,i} \quad (19)$$

3. The weight of ith fraction crystals was calculated by Eq. (6) as follows.

$$w_{i,t+\Delta t} = w_{i,t} - \Delta C_{b,i} V \quad (20)$$

The size of ith fraction crystals L_i was calculated by Eq. (21):

$$L_i = \left(\frac{6 w_{i,t+\Delta t}}{\pi \rho N_i}\right)^{1/3} \quad (21)$$

These three calculation steps were repeated as dissolution progressed. At a given dissolution time, the partially dissolved crystals were re-classified into 50 fractions and the CSD was calculated by Eq. (17).

4. Results and discussion

4.1. Dissolution of monodisperse crystals and estimation of dissolution rate constant k

The changes in the bulk concentration C_b at 30 °C are presented in Fig. 2 as a function of time for monodisperse crystals of L-aspartic acid with L of 200 μm with the agitation rate as parameter. The dissolution rate increased with an increase in agitation rate up to 500 rpm, but not when the agitation was in excess of 500 rpm. The dissolution model presented in Fig. 1 can explain this result; namely, for agitation rates less than 500 rpm the dissolution rate is strongly affected by a mass transfer process, but at agitation rates higher than 500 rpm the mass transfer resistance becomes negligible. A fit of the experimental value was attempted to determine the dissolution rate constant k.

The solid curves in Fig. 2 are the values calculated from Eq. (16), which are consistent with the experimental values. In those calculations, we used the solubility C_{sol} of L-aspartic acid experimentally obtained, which was expressed as a function of the absolute temperature T (between 278 and 333 K), as follows:

$$C_{sol} = 1.76 \times 10^{-4} \exp(3.44 \times 10^{-2} T) \quad (22)$$

The solubility calculated by Eq. (22) has an associated error of 3.5%.

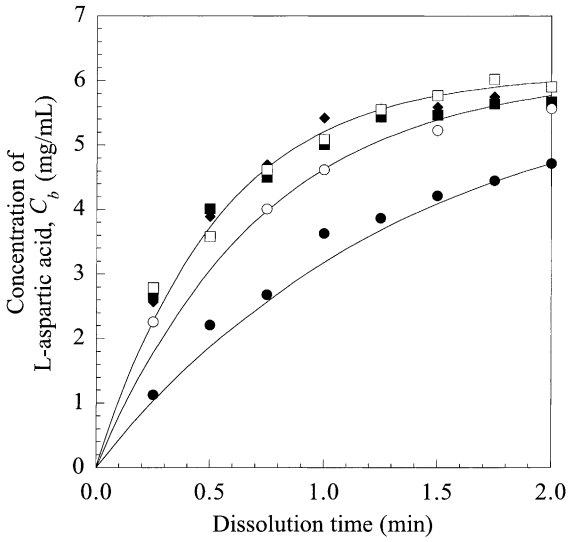

Fig. 2. Dissolution of L-aspartic acid crystals in water at 30 °C. Agitation rate (rpm): (●) 200; (○) 300; (□) 500; (■) 800; (◆) 1200. The curves are the best fit according to Eq. (16).

The values of the dissolution rate constant k determined here are presented in Fig. 3. According to Eq. (5), for an increase in agitation rate, the value of k should approach the value of k_d. This is because the diffusion layer becomes thinner as the agitation is increased and the value of $1/k_{dif}$ becomes negligible compared to the value of $1/k_d$. Consequently, the k value obtained for agitation rates greater than 500 rpm represents the k_d value.

Dissolution processes for L-aspartic acid crystals of different sizes at 45 °C and 500 rpm are shown in Fig. 4. The solid curves in Fig. 4 show the calculated values obtained by fitting with Eq. (16), which trace well the experimental values. Values of k_{obs} and k obtained by the fitting are given

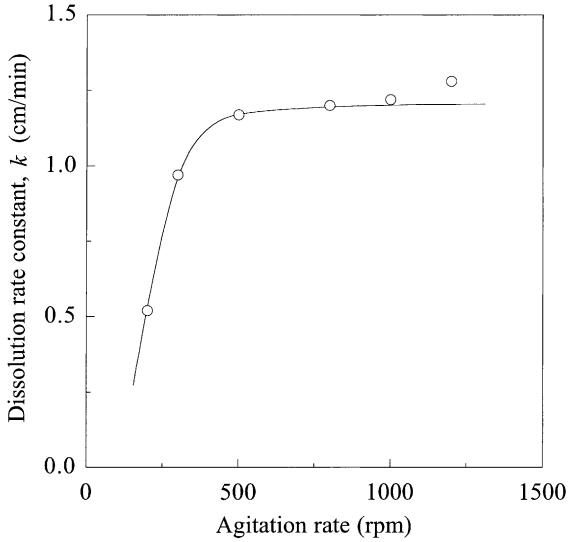

Fig. 3. The relationship between the k and agitation rate.

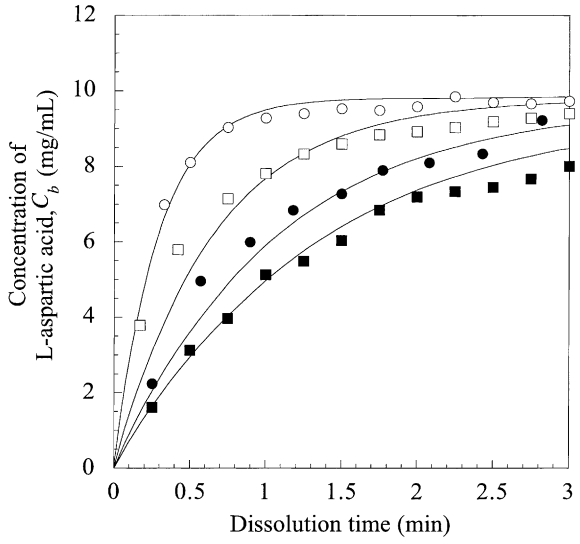

Fig. 4. Dissolution of L-aspartic acid crystals in water at 45 °C and 500 rpm. Initial size of crystals, L (μm): (○) 90; (□) 200; (●) 360; (■) 460. The curves are the best fit according to Eq. (16).

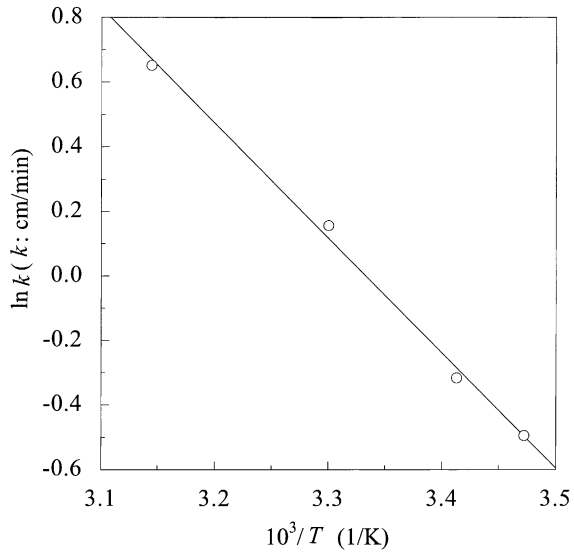

Fig. 5. Arrhenius plots for dissolution rate constant k of L-aspartic acid crystals at 500 rpm. In the present conditions, the k value represents the k_d value.

in Table 1. Values of k_{obs} decreased with an increase in crystal size, indicating that small crystals dissolve more rapidly. However, the k values, i.e. k_d values, are almost the same within a margin of error of 3.1%. This result indicates that the rate of disintegration of L-aspartic acid molecules from the crystal surface does not depend on the size of crystals, at least for those crystals with L in the range from 90 to 460 μm.

The effect of temperature on the dissolution rate is also presented in Table 1. The dissolution was also carried out at 500 rpm in order to prevent any additional effect of mass transfer limitations on the dissolution rate. It was found that dissolution became slower as the temperature decreased. The activation energy of the disintegration process was determined to be 29.6 kJ mol^{-1} from an Arrhenius plot of k values shown in Fig. 5.

4.2. Dissolution of polydisperse crystals of L-aspartic acid and simulation of the change in CSD

The dissolution of L-aspartic acid crystals with a broad CSD was carried out, and the CSD was measured. As

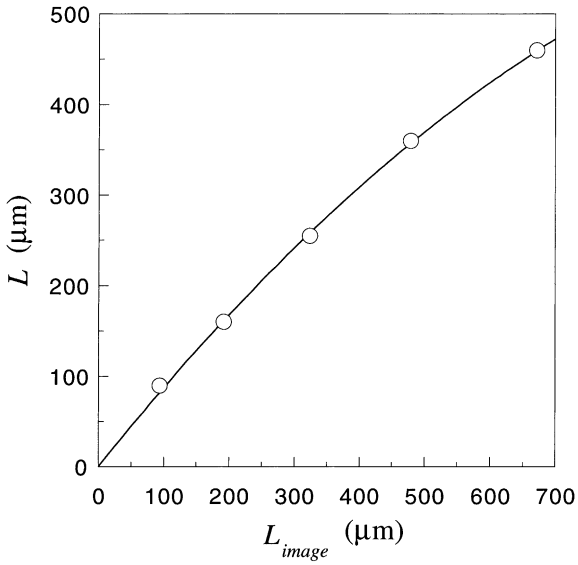

Fig. 6. The relationship between L and L_{image}.

Table 1
The kinetic parameters determined from dissolution of monodisperse crystals of L-aspartic acid (k_{obs}: cm^2 min^{-1} mg$^{-2/3}$; k: cm min^{-1})

Size, L (μm)	15 °C		20 °C		30 °C		45 °C	
	k_{obs}	k	k_{obs}	k	k_{obs}	k	k_{obs}	k
90	0.57	0.61	0.66	0.70	1.07	1.14	1.77	1.89
200	0.25	0.59	0.30	0.71	0.51	1.21	0.78	1.84
360	0.14	0.58	0.17	0.73	0.28	1.19	0.47	2.01
460	0.12	0.66	0.13	0.76	0.21	1.14	0.36	1.96
k_d (average)	0.61 ± 0.03		0.73 ± 0.02		1.17 ± 0.03		1.93 ± 0.06	

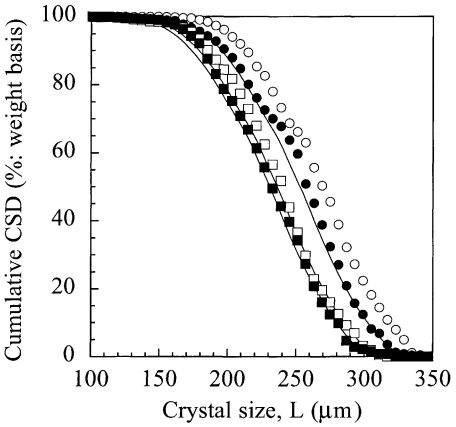

Fig. 7. Simulation of the changes of cumulative CSD during dissolution. Marks represent the experimental values and the solid curve represents the simulated values. Dissolution time (min): (○) zero; (●) 0.5; (□) 1.5; (■) 3.0.

mentioned above, we measured the CSD by image analysis. The size L obtained by sieving was different from the size L_{image} by image analysis. Fig. 6 shows that L is smaller than L_{image}. In the present study, the crystal size L_{image} was converted to L by using the following calibration equation.

$$L = L_{\text{image}}(-3.24 \times 10^{-4} L_{\text{image}} + 9.01 \times 10^{-1}) \qquad (23)$$

Fig. 7 shows the changes of size distribution of L-aspartic acid crystals during the dissolution, where the open circles represent the initial CSD. The solid curves in Fig. 7 show the CSD simulated by the method described in Section 3.6 using a value for k of $0.907\,\text{cm}\,\text{s}^{-1}$. Fig. 8 shows the change in the concentration of L-aspartic acid, C_b, during the dissolution of polydisperse crystals, where the symbols represent the experimental values and the solid curve represents the calculated values through the simulation of the change

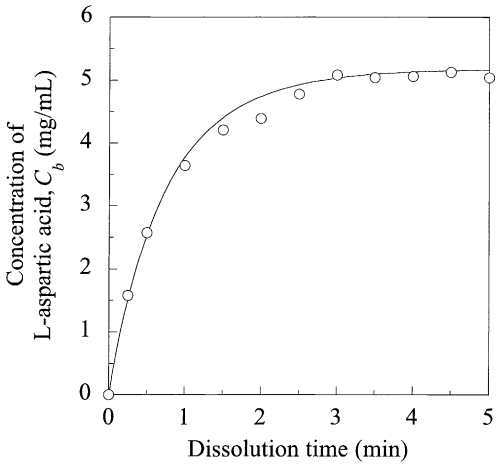

Fig. 8. Simulation of dissolution of polydisperse crystals of L-aspartic acid in water at 25 °C. Marks represent the experimental values and the solid curve represents the simulated values.

of CSD. Figs. 7 and 8 show the good agreement between simulated and experimental results, and the findings thus show that the dissolution kinetics presented here help us to understand the dissolution behavior of crystals with a broad CSD.

5. Conclusions

We have presented here an investigation of dissolution kinetics that can be used for analyzing the dissolution of crystals suspended under agitation. The dissolution rate equation (Eq. (13)) was derived by taking into account the disintegration of molecules at the surface of the crystal and mass transfer. Furthermore, an intrinsic expression of the change in C_b during dissolution was derived (Eq. (16)). When L-aspartic acid crystals of a given size were dissolved under agitation, the dissolution rate increased with an increase in the agitation rate, but reached an upper limit. It was found that the smaller the crystals, the faster was the dissolution rate. The dissolution rate equation derived in the present study was able to closely describe the experimentally observed dissolution characteristics. Furthermore, it was shown that the disintegration rate constant of L-aspartic acid, k_d, depends on dissolution temperature (the activation energy is $29.6\,\text{kJ}\,\text{mol}^{-1}$), but does not depend on the crystal size. Based on the dissolution kinetics, the dissolution rate of L-aspartic acid crystals with a broad CSD and the change of CSD during the dissolution were simulated with good accuracy. The dissolution kinetics presented here should be useful for designing the industrial crystallization processes under agitation for the production of large crystals with a narrow CSD by removing fine crystals.

References

[1] G. Shan, K. Igarashi, H. Noda, H. Ooshima, Production of large crystals with a narrow crystal size distribution by a novel WWDJ batch crystallizer, Chem. Eng. J. 85 (2002) 161–167.
[2] A. Tromelin, S. Habillon, C. Andres, Y. Poureclot, B. Chaillot, Relationship between particle size and dissolution rate of bulk powders and sieving characterized fractions of two qualities of orthoboric acid, Drug Dev. Ind. Pharm. 22 (1996) 977.
[3] A. S. Myerson, Handbook of Industrial Crystallization, Butterworths/Heinemann, Boston, 1993.
[4] A.A. Noyes, W.R. Whitney, The rate of solution of solid substances in their own solutions, J. Am. Chem. Soc. 19 (1897) 930.
[5] J.B. Dressman, D. Fleisher, Mixing-tank model for predicting dissolution rate control of oral absorption, J. Pharm. Sci. 75 (1986) 109.
[6] R.J. Hintz, K.C. Johnson, The effect of particle size distribution on dissolution rate and oral absorption, Int. J. Pharm. 51 (1989) 9.
[7] A.T.K. Lu, M.E. Frisella, K.C. Johnson, Dissolution modeling: factors affecting the dissolution rates of polydisperse powders, Pharm. Res. 10 (1993) 1308.
[8] D. Brooke, Sieve cuts as monodisperse powder in dissolution studies, J. Pharm. Sci. 64 (1975) 1409.